electronics

MDPI

Article

Effects of the Particle Size and the Solvent in Printing Inks on the Capacitance of Printed Parallel-Plate Capacitors

Sungsik Park and Dongjin Lee *

Department of Mechanical Design and Production Engineering, Konkuk University, 120, Neungdong-ro, Gwangjin-gu, Seoul 143-701, Korea; sungsik.fdrc@gmail.com

* Correspondence: djlee@konkuk.ac.kr; Tel.: +82-2-450-0452; Fax: +82-2-447-5886

Academic Editor: Hyun Wook Kang

Received: 30 November 2015; Accepted: 22 January 2016; Published: 2 February 2016

Abstract: Parallel-plate capacitors were fabricated using a printed multi-layer structure in order to determine the effects of particle size and solvent on the capacitance. The conductive-dielectric-conductive layers were sequentially spun using commercial inks and by intermediate drying with the aid of a masking polymeric layer. Both optical and scanning electron microscopy were used to characterize the morphology of the printed layers. The measured capacitance was larger than the theoretically calculated value when ink with small-sized particles was used as the top plate. Furthermore, the use of a solvent whose polarity was similar to that of the underlying dielectric layer enhanced the penetration and resulted in an increase in capacitance. The functional resistance-capacitance low-pass filter was implemented using printed resistors and capacitors, a process that may be scalable in the future.

Keywords: spin printing; multi-layer printing; solution polarity; printed capacitor; RC low pass filter

1. Introduction

Printed electronics are attracting research interest because they have many advantages, such as ease of manufacturing (using solution-based materials and an adaptable roll-to-roll process), low cost, and eco-friendly processing [1–4]. There have been many attempts to fabricate electronic devices using printing techniques, including organic photovoltaic cells [5], organic thin film transistors [6], radio frequency identification tags [7], organic light emitting diodes [8], and printing-based sensors [9].

Such printed devices typically have a multi-layer structure, called a "sandwich structure". Each layer in multi-layer devices consists of a different material that depends on its function. For example, a conductive layer may use Ag or Cu, an insulating layer may use polymethyl methacrylate (PMMA), $BaTiO_3$, or Epoxy, and a semiconducting layer may use poly-3-hexylthiophene-2,5-diyl: phenyl-C61-butyric acid methyl ester (P3HT:PCBM) or triisopropylsilyl (TIPS) pentacene [10–13]. Each functional layer shows various characteristics, and the device types are determined when the layers are overlaid in different sequences in the multi-layer structure. The main performance parameters measured include the electrical resistivity of conductive patterns, the permittivity of the dielectric layer, the mobility of the semiconducting layer, and mechanical properties, such as the thickness and roughness of the printed surface [14–16].

The chemical properties of solutions can be enhanced by changing the synthesis methods and materials, but the mechanical properties depend on the printing technique, which determines the morphology of the surface. In particular, the morphology of a printed layer changes rapidly when the multi-layer structure is printed. Specifically, thickness variations accumulate as printed layers are added. Furthermore, the morphology at the interface in a multi-layer structure can be changed by the

dissolution caused by the solvent in the ink that occurs at the interface between the printed layers. A rough printed surface can also affect the performance and reliability of the device [17,18].

In this study, a parallel-plate capacitor was selected as an example device to observe the interfacial phenomena that affect the device performance. A printed capacitor has a simple multi-layer structure that sequentially overlaps the substrate with a conductive layer, a dielectric, and another conductive layer. Previous studies have used many fabrication techniques, such as screen printing, inkjet printing, and gravure printing [19–21] to fabricate printed capacitors. The spin printing process, which guarantees good uniformity, was used to make the printed capacitor devices for this study. In order to investigate the influence of various parameters on the coating quality and capacitance of the multi-layer structure, the capacitors were printed using two kind types of commercial Ag conductive ink, each of which has different material particle sizes and vehicle solvent. The printed capacitors were then analyzed and compared using both theoretical and experimental approaches. To observe the functionality, the printed capacitors were configured in a low-pass filter (LPF) implementation. Correlations between the process conditions and functionality were discussed.

2. Experimental Section

2.1. Materials and Method

Borosilicate glass substrate, 30 mm × 30 mm in size, was cleaned with acetone, isopropyl alcohol (IPA), and distilled water, and dried with N_2 gas. For the bottom plate, a conductive layer (the first layer) was spun at 4000 rpm for 10 s using two types of commercial Ag conductive ink (FLT-710GO, FP Co., Korea and PG-007, Paru Co., Busan, Korea) onto the glass substrate, followed by drying in a convection oven at 95 °C for 5 min. A commercial dielectric ink (PD-100, Paru Co., Suncheon, Korea) that has a permittivity of 121 pF/m was used to fabricate the second layer. The spin speeds of the second layer were 3000, 4000, and 5000 rpm for 10 s, followed by drying in a conduction oven at 95 °C for 5 min. The top plate (the third layer) was printed using the same process and parameters as for the first layer.

When the inks were spun, a polyimide (PI) film patterned by a cutting plotter (Craft ROBO CC330-20, Graphtec Co., Yokohama, Japan) was placed on the substrate and played the role of mask shown in Figure 1. After spin-coating, PI mask was detached.

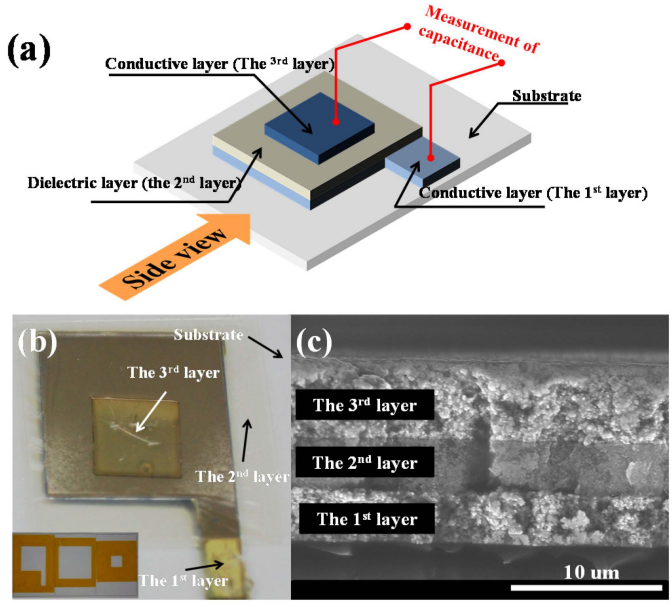

Figure 1. Printed parallel-plate capacitor: (**a**) 3D schematics; (**b**) optical image (inset is polyimide masks for patterning); and (**c**) cross-sectional SEM image.

2.2. Measurement

In order to measure the printability and functionality of the printed parallel-plate capacitors, the surface morphology, thickness, and roughness of the printed conductive and dielectric layers were characterized using an optical microscope (ECLIPSE LV100ND, Nikon Ins. Co., Tokyo, Japan), a field emission scanning electron microscope (FESEM, S-4800, Hitachi Co., Tokyo, Japan), and an interferometer (NV-2000, Nano System Co., Daejeon, Korea), respectively. The contact angles of dielectric inks used as the second layer on top of two kinds of the first conductive layers were measured using a contact angle meter (GSA, Surface Tech., Gyeonggi, Korea). The capacitance of the fabricated capacitors was measured using a digital multimeter (UT70D, UNI-Trend Co., Hong Kong, China).

A resistor-capacitor low pass filter (RC LPF) was built using a printed resistor on a PI substrate and a fabricated capacitor on a glass substrate. The LPF circuit was constructed on a breadboard with electrical wiring. An alternating current (AC) signal was supplied by a function generator (8116A, Hewlett-Packard, Palo Alto, CA, USA), and the input and output voltages were measured using a digital oscilloscope (DS1052E, RIGOL Co., Beijing, China). The cutoff frequency and input-output ratio were first theoretically calculated and then verified by experiment.

3. Results and Discussion

The parallel-plate capacitor fabricated in this study is demonstrated in Figure 1. As shown in Figure 1a, the capacitor consisted of three layers (conductive-dielectric-conductive), each with a defined area and thickness. The first layer had an area of 100 mm^2 with a contact line for measuring capacitance. The second layer covered the first layer completely, excluding the contact line. Finally, the third layer acted as the top plate, and was spun onto the second layer with an area of 49 mm^2. An optical image of the printed capacitor is shown in Figure 1b. The thickness of the dielectric layer was inspected by cross-sectional SEM, as shown in Figure 1c, and was found to be 4.41, 4.16, and 2.97 μm when the spinning speed was 3000, 4000, and 5000 RPM, respectively.

The surface morphology of the second layer was characterized using optical microscopy, and was found to be dependent on the first layer. As shown in optical images of Figure 2, the dielectric layer did not perfectly cover the underlying layer when FLT-710GO was used as the first layer, while it did fully cover the first layer when PG-007 was used. The uncoated surface shown in Figure 2a played the role of charge carrier conduction between the top and bottom plates, meaning the failure as a capacitor.

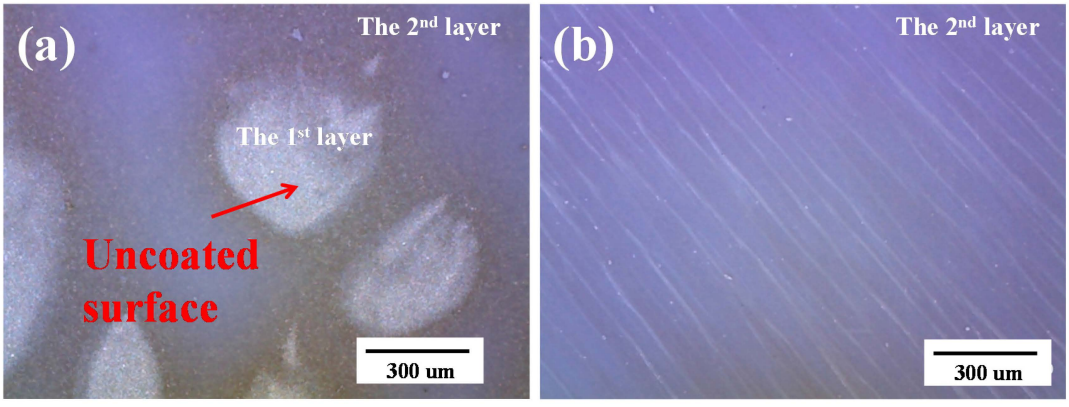

Figure 2. Optical images of the second layer when the first layer was (**a**) FLT-710GO and (**b**) PG-007.

Figure 3 depicts SEM images of the first layer with FLT-710GO and PG-007. The sizes of the silver particles in Figure 3a,b were about 1000 nm and 70 nm, respectively. In addition, aggregations of silver particles larger than several micrometers were observed, and these affected the quality of the subsequent dielectric layers. When the particle sizes were smaller and there was no aggregation, the layers could be stacked more densely, which reduced surface waviness and roughness, and lead

to good quality subsequent layers. Furthermore, it is known that the contact angle on the surface increases when the roughness becomes high [22]. The root mean square (RMS) roughness of the first layer was measured to be 153 nm and 9.53 nm for FLT-710GO and PG-007, respectively. The measured contact angle of the dielectric ink on the first layer for FLT-710GO and PG-007 was 65.1° and 50.8°, respectively. Both the existence of aggregations and the wettability influenced the fabrication of the stable thin film second layer on top of the first layer. For this reason, PG-007 conductive ink was used to construct the bottom plate in all of the parallel-plate capacitors. However, two types of conductive ink were still used to fabricate the top plates.

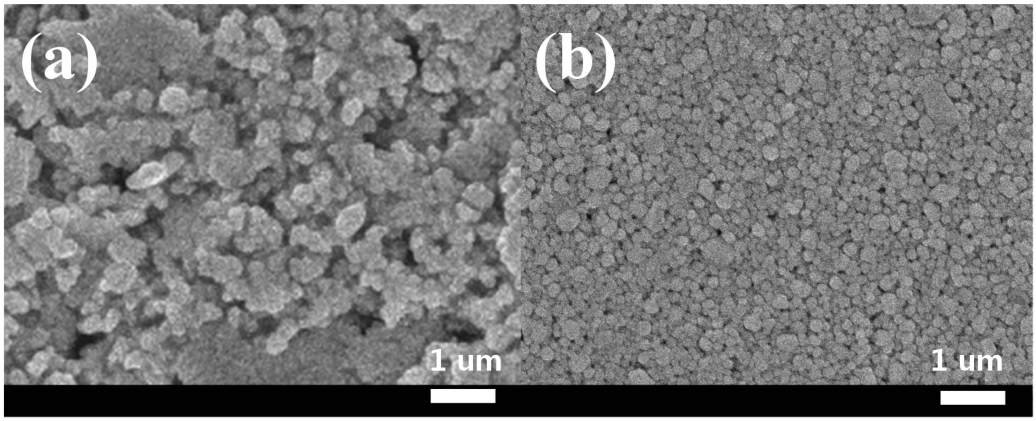

Figure 3. SEM images of bottom plate composed of silver particles using (**a**) FLT-710GO and (**b**) PG-007.

The measured and theoretical capacitances (*C*) of the fabricated parallel-plate capacitors are shown in Figure 4. The theoretical capacitance was obtained from Equation (1).

$$C = \varepsilon \frac{A}{t} \tag{1}$$

where ε represents permittivity; and A and t are geometric parameters that represent the area and thickness, respectively, of the dielectric layer.

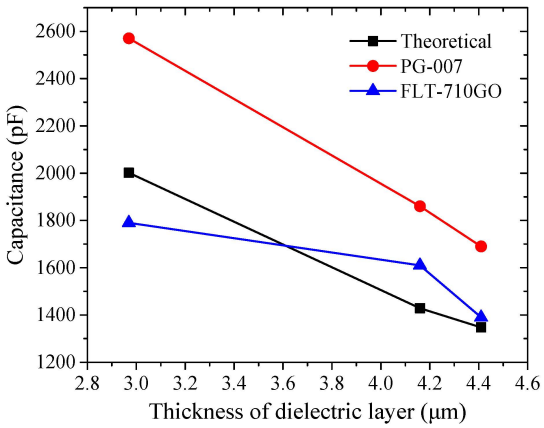

Figure 4. Theoretical and measured capacitance of fabricated parallel-plate capacitors *versus* the thickness of the dielectric layer.

As shown in Figure 4, the capacitance decreases as the thickness of the dielectric layer increases, which is consistent with Equation (1). In particular, the capacitor that used PG-007 as the top plate exhibited an inverse linear relationship to the thickness. It should be noted that the experimental values are a bit higher than the theoretical calculation. This might be caused by the penetration of

silver particles into the dielectric layer whose particle size was around 40 nm, which reduces the effective thickness of the layer and results in higher capacitance. In addition, the uneven boundary between the layers tends to concentrate the charges, which also increases the capacitance. In contrast, the capacitor that used FLT-710GO as the top plate showed capacitance that was close to the theoretical calculation and lower than the capacitors that used PG-007 as a top plate. Particles from the top plates did not penetrate into the dielectric layers because the particles were large and many formed aggregations. Another possible cause for the differences in capacitance is the effect of the vehicle solvent used in each ink. The solvent used in the FLT-710GO, PG-007, and PD-100 inks is dibutyl diglycol (C_4H_9O-$(CH_2CH_2O)_2$-C_4H_9) (solubility in water: 6.5%), ethylene glycol ($HOCH_2CH_2OH$) (solubility in water: 100%), and diethylene glycol monoethyl ether acetate ($C_2H_5OCH_2CH_2OCH_2CH_2CO_2CH_3$) (solubility in water: 100%), respectively. The polarity of the solvent in the FLT-710GO ink is farther away from that in the PD-100 ink than polarity of solvent in PG-007 ink. It means that the possibility of silver particles in the top plate percolating into the dielectric layer via the solvent is high when PG-007 is used.

An RC LPF was implemented using both printed resistors and capacitors employing PG-007, as shown in Figure 5. Figure 5a shows the measurement setup for the RC LPF circuit. Based on the measured values of 420 Ω and 1530 pF, Figure 5b shows a comparison of the theoretical and experimental values for the input-output voltage ratio. The theoretical values for the input-output voltage ratio and the cutoff frequency were calculated using Equations (2) and (3), respectively [23].

$$\frac{|V_{out}|}{|V_{in}|} = \frac{1}{\sqrt{1+\left(\frac{1}{RC\omega}\right)^2}} \tag{2}$$

$$f_c = \frac{1}{2\pi RC} \tag{3}$$

where R and C are the resistance and capacitance of the passive elements, respectively, and V and ω are the voltage and frequency of the applied AC signals. The voltage ratio decreases gradually as the frequency increases for all frequencies below the cut-off frequency, which is the behavior of a conventional LPF. The actual cutoff frequency was measured to be 295 kHz, and is comparable to the calculated cutoff frequency of 247 kHz.

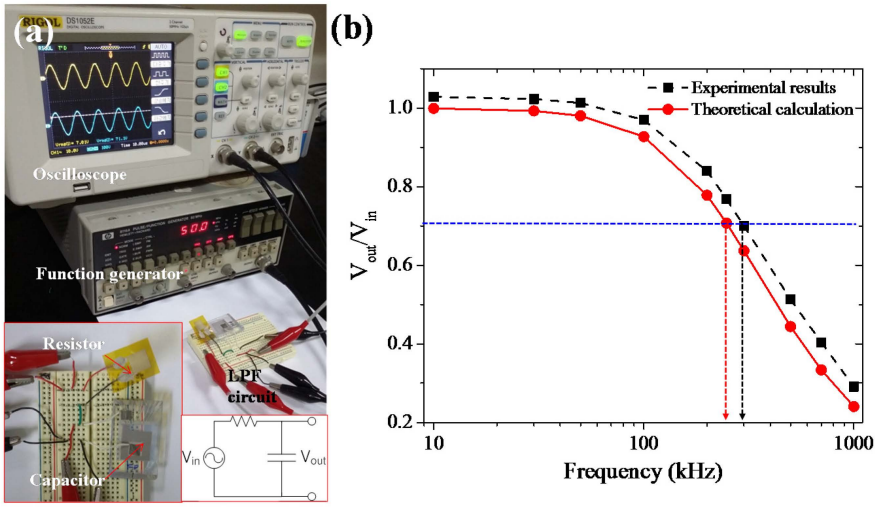

Figure 5. Implementation of an resistor-capacitor low pass filter(RC LPF) using printed resistors and printed parallel-plate capacitors: (**a**) experimental set-up for measurements (inset: the wiring and schematic of the circuit); and (**b**) the input-output voltage ratio in the case where the printed capacitor used PG-007 as the top plate.

4. Conclusions

In summary, capacitors were fabricated using a multi-layer printing process to verify the effects of the particle size and the solvent in printing inks on capacitance. It was found that the effective thickness of the dielectric layer decreased when ink with smaller particles was used and when the polarity of the solvent in the ink was similar to that of the underlying layers. Changes in the effective thickness were observed via a capacitance measurement. In addition, an RC LPF was implemented in order to verify the functionality of the printed resistors and capacitors. The behavior using these printed elements was similar to that of a conventional LPF. The interfacial phenomenon explained in this study may be applicable when building other multi-layer devices.

Acknowledgments: This research was supported by Basic Science Research Programs (2015R1C1A1A02037326 and NRF-2010-00525) through the National Research Foundation of Korea (NRF) and funded by the Ministry of Science, ICT & Future Planning, and by the Ministry of Education. The authors also acknowledge the Nano-Material Technology Development Program through the National Research Foundation of Korea (NRF) funded by the Ministry of Science, ICT, and Future Planning (2009-0082580).

Author Contributions: Sungsik Park designed and performed the experiments in this study, took SEM and optical images of the experimental results, and wrote the manuscript. Dongjin Lee directed this study, wrote the manuscript, and provided explanations of the phenomena observed.

Conflicts of Interest: The authors declare that there is no conflict of interest.

References

1. Li, Z.; Zhang, R.; Moon, K.-S.; Liu, Y.; Hansen, K.; Le, T.; Wong, C.P. Highly conductive, flexible, polyurethane-based adhesives for flexible and printed electronics. *Adv. Funct. Mater.* **2013**, *23*, 1459–1465. [CrossRef]
2. Ho Anh Duc, N.; Changwoo, L.; Kee-Hyun, S.; Dongjin, L. An investigation of the ink-transfer mechanism during the printing phase of high-resolution roll-to-roll gravure printing. *Compon. Packag. Manuf. Technol. IEEE Trans.* **2015**, *5*, 1516–1524.
3. Lee, J.; Park, S.; Park, J.; Cho, Y.; Shin, K.-H.; Lee, D. Analysis of adhesion strength of laminated copper layers in roll-to-roll lamination process. *Int. J. Precis. Eng. Manuf.* **2015**, *16*, 2013–2020. [CrossRef]
4. Lee, J.; Seong, J.; Park, J.; Park, S.; Lee, D.; Shin, K.-H. Register control algorithm for high resolution multilayer printing in the roll-to-roll process. *Mech. Syst. Signal Process.* **2015**, *60–61*, 706–714. [CrossRef]
5. Krebs, F.C.; Fyenbo, J.; Jorgensen, M. Product integration of compact roll-to-roll processed polymer solar cell modules: Methods and manufacture using flexographic printing, slot-die coating and rotary screen printing. *J. Mater. Chem.* **2010**, *20*, 8994–9001. [CrossRef]
6. Seungjun, C.; Seul Ong, K.; Kwon, S.-K.; Changhee, L.; Yongtaek, H. All-inkjet-printed organic thin-film transistor inverter on flexible plastic substrate. *Electron Device Lett. IEEE* **2011**, *32*, 1134–1136.
7. Choi, E.; Park, J.; Kim, B.; Lee, D. Fabrication of electrodes and near-field communication tags based on screen printing of silver seed patterns and copper electroless plating. *Int. J. Precis. Eng. Manuf.* **2015**, *16*, 2199–2204. [CrossRef]
8. Kim, K.; Kim, G.; Lee, B.R.; Ji, S.; Kim, S.-Y.; An, B.W.; Song, M.H.; Park, J.-U. High-resolution electrohydrodynamic jet printing of small-molecule organic light-emitting diodes. *Nanoscale* **2015**, *7*, 13410–13415. [CrossRef] [PubMed]
9. Lupo, D.; Clemens, W.; Breitung, S.; Hecker, K. OE-A roadmap for organic and printed electronics. In *Applications of Organic and Printed electronics*; Cantatore, E., Ed.; Springer US: Secaucus, NJ, USA, 2013; pp. 1–26.
10. Vedraine, S.; El Hajj, A.; Torchio, P.; Lucas, B. Optimized ito-free tri-layer electrode for organic solar cells. *Org. Electron.* **2013**, *14*, 1122–1129. [CrossRef]
11. Cho, S.Y.; Ko, J.M.; Lim, J.; Lee, J.Y.; Lee, C. Inkjet-printed organic thin film transistors based on tips pentacene with insulating polymers. *J. Mater. Chem. C* **2013**, *1*, 914–923. [CrossRef]
12. Jung, M.; Kim, J.; Koo, H.; Lee, W.; Subramanian, V.; Cho, G. Roll-to-roll gravure with nanomaterials for printing smart packaging. *J. Nanosci. Nanotechnol.* **2014**, *14*, 1303–1317. [CrossRef]

13. Yi, M.; Yeom, D.; Lee, W.; Jang, S.; Cho, G. Scalability on roll-to-roll gravure printed dielectric layers for printed thin film transistors. *J. Nanosci. Nanotechnol.* **2013**, *13*, 5360–5364. [CrossRef] [PubMed]
14. Ho Anh Duc, N.; Jongsu, L.; Chung Hwan, K.; Kee-Hyun, S.; Dongjin, L. An approach for controlling printed line-width in high resolution roll-to-roll gravure printing. *J. Micromechanics Microengineering* **2013**, *23*, 095010.
15. Seong, J.; Kim, S.; Park, J.; Lee, D.; Shin, K.-H. Online noncontact thickness measurement of printed conductive silver patterns in roll-to-roll gravure printing. *Int. J. Precis. Eng. Manuf.* **2015**, *16*, 2265–2270. [CrossRef]
16. Park, J.; Nguyen, H.A.D.; Park, S.; Lee, J.; Kim, B.; Lee, D. Roll-to-roll gravure printed silver patterns to guarantee printability and functionality for mass production. *Curr. Appl. Phys.* **2015**, *15*, 367–376. [CrossRef]
17. Wu, X.; Lenhert, S.; Chi, L.; Fuchs, H. Interface interaction controlled transport of cdte nanoparticles in the microcontact printing process. *Langmuir* **2006**, *22*, 7807–7811. [CrossRef] [PubMed]
18. Rapp, L.; Nénon, S.; Alloncle, A.P.; Videlot-Ackermann, C.; Fages, F.; Delaporte, P. Multilayer laser printing for organic thin film transistors. *Appl. Surf. Sci.* **2011**, *257*, 5152–5155. [CrossRef]
19. Garnier, F.; Hajlaoui, R.; Yassar, A.; Srivastava, P. All-polymer field-effect transistor realized by printing techniques. *Science* **1994**, *265*, 1684–1686. [CrossRef] [PubMed]
20. Liu, Y.; Cui, T.; Varahramyan, K. All-polymer capacitor fabricated with inkjet printing technique. *Solid-State Electron.* **2003**, *47*, 1543–1548. [CrossRef]
21. Vaklev, N.L.; Müller, R.; Muir, B.V.O.; James, D.T.; Pretot, R.; van der Schaaf, P.; Genoe, J.; Kim, J.-S.; Steinke, J.H.G.; Campbell, A.J. High-performance flexible bottom-gate organic field-effect transistors with gravure printed thin organic dielectric. *Adv. Mater. Interfaces* **2014**. [CrossRef] [PubMed]
22. Marmur, A. Wetting on hydrophobic rough surfaces: To be heterogeneous or not to be? *Langmuir* **2003**, *19*, 8343–8348. [CrossRef]
23. Sedra, A.S.; Smith, K.C. *Microelectronic Circuits*; Oxford University Press: Oxford, UK, 1998; Volume 1.